Bull Volcanol (2012) 74:325–339
DOI 10.1007/s00445-011-0519-3

RESEARCH ARTICLE

Precursors to dyke-fed eruptions at basaltic volcanoes: insights from patterns of volcano-tectonic seismicity at Kilauea volcano, Hawaii

Andrew F. Bell · Christopher R. J. Kilburn

Received: 25 May 2010 / Accepted: 14 June 2011 / Published online: 10 August 2011

Abstract To investigate the physical controls on volcano-tectonic (VT) precursors to eruptions and intrusions at basaltic volcanoes, we have analyzed the spatial and temporal patterns of VT earthquakes associated with 34 eruptions and 23 dyke intrusions that occurred between 1960 and 1983 at Kilauea, in Hawaii. Eighteen of the 57 magmatic events were preceded by an acceleration of the mean rate of VT earthquakes located close to the main shallow magma reservoir. Using a maximum-likelihood technique and the Bayesian Information Criterion for model preference, we demonstrate that an exponential acceleration is preferred over a power-law acceleration for all sequences. These sequences evolve over time-scales of weeks to months and are consistent with theoretical models for the approach to volcanic eruptions based on the growth of a population of fractures in response to an excess magma pressure. Among the remaining 40 magmatic events, we found a significant correlation between swarms of VT earthquakes located in the mobile south-flank of Kilauea and eruptions and intrusions. The behaviour of these swarms suggests that at least some of the magmatic events are triggered by transient episodes of elevated rates of aseismic flank movement, which could explain why many eruptions and intrusions are not preceded by longer-term precursory signals. In none of the 57 cases could a precursory sequence be used to distinguish between the approach to an eruption or an intrusion, so that, even when a precursory sequence is recognized, there remains an empirical chance of about 40% (24 intrusions from 57 magmatic events) of issuing a false alarm for an imminent eruption.

Keywords Volcano-tectonic earthquakes · Eruption forecasting · Basaltic volcanism · Dyke intrusion · Volcano flank instability

Editorial responsibility: H. Delgado Granados

A. F. Bell (✉)
School of GeoSciences, The University of Edinburgh,
Grant Institute,
The King's Buildings, West Mains Road,
Edinburgh EH9 3JW, UK
e-mail: a.bell@ed.ac.uk

C. R. J. Kilburn
Aon Benfield UCL Hazard Centre, Department of Earth Sciences,
University College London,
Gower Street,
London WC1E 6BT, UK

Introduction

Volcanic eruptions are commonly preceded by changes in the rate, location or statistics of local volcano-tectonic (VT) earthquakes (Tokarev 1971; Voight 1988; McNutt 1996; Kilburn and Voight 1998; De la Cruz-Reyna and Reyes-Davila 2001; Reyes-Davila and De la Cruz-Reyna 2002; Kilburn 2003; Moran 2003; Sparks 2003; e.g., Zobin 2003; Roman and Cashman 2006; Smith et al. 2007; Lengliné et al. 2008; Bell et al. 2011). Of special interest have been accelerations in the mean and peak rates of VT earthquakes with time because they have the potential for enabling short-term forecasts of when an eruption will occur (Voight 1988; McGuire and Kilburn 1997; Kilburn and Voight 1998; Main 2000; Chastin and Main, 2003; Collombet et al. 2003; Kilburn 2003). As encapsulated in the model of Voight (1988), these accelerations in VT earthquake rate are often anticipated to follow exponential or power-law trends. Distinguishing the form of the trend is in turn important for constraining the predictability of an eruption (Voight 1988) and for identifying the physical processes underlying deformation (McGuire and Kilburn 1997; Kilburn and Voight 1998).

At subduction-zone volcanoes, VT earthquakes can establish the final trend in their accelerating rate ~10 days before eruption (Kilburn 2003). However, such prolonged accelerations are not ubiquitous and, in particular, basaltic eruptions at volcanoes in extensional stress fields can begin after hours or less of elevated seismicity (Klein 1984; Soosalu et al. 2005).

In this paper, we analyze the patterns of VT seismicity associated with volcanic activity at Kilauea volcano, Hawaii, where a well-established seismic monitoring network has recorded tens of eruptions and intrusions. Although studies have previously investigated the pre-eruptive rates of VT earthquakes at Kilauea, these have concentrated either on the aggregate trends obtained after averaging over numerous pre-eruptive sequences (Chastin and Main 2003) or on very long-term trends evolving over many years and spanning several eruptive episodes (Lengliné et al. 2008). Here, we focus on the temporal evolution of seismicity in different parts of the volcanic edifice before individual eruptions and intrusions.

We recognise three types of precursory VT earthquake sequence and suggest that they form part of a spectrum of behaviour that includes interaction between Kilauea's summit caldera and mobile south flank. Our analysis also shows that, when prolonged accelerations occur in precursory VT earthquake rate, the increase in mean rate is best modelled with an exponential function and, in agreement with the study of Klein et al. (1987a, b), displays no discernable differences between the approach to eruptions or intrusions. Altogether, the results provide a basis for establishing limits on the reliability of short-term forecasts of eruptions on Kilauea and for identifying new strategies for improving forecasting methods.

VT earthquakes at Kilauea

Selection of data

Although Kilauea has been in virtually continuous eruption since the start of the Pu'u O'o eruption in 1983, its prior activity was characterized by frequent, episodic eruptions and dyke intrusions without eruptions (Klein et al. 1987a, b). The archetypal model for such eruptions and intrusions involves the rapid release of magma from a shallow reservoir, located at depths of 3–5 km below the summit caldera, into one or both of two rift-zones located on the east and south-west flanks (Fig. 1; Klein et al. 1987a, b; Tilling and Dvorak 1993). The rift-zones are regions of localized extension that separate the stable interior of the island from the mobile south flank, which is moving seaward at rates of as much as 40 cm year^{-1} (Delaney et al. 1998).

Our study focuses on the distribution with time and location of VT earthquakes at Kilauea between 1 January 1960 and the Pu'u O'o eruption in 1983, during which time 34 eruptions and 23 intrusions were recorded (Klein 1984; Klein et al. 1987a, b). The VT seismicity was detected by the monitoring network of the Hawaiian Volcano Observatory (Nakata, 2006). The sensitivity of the network was enhanced several times between 1960 and 1983 and accounts for the increasing numbers of small-magnitude earthquakes appearing in the catalogue in more recent times (Fig. 2). As a result, the magnitude completeness of the catalogue has also changed with time (as well as with location, because enhancements occurred progressively across the network) and, if not taken into account, can lead to spurious changes being identified in the patterns of earthquake occurrence. In this study, we have identified the cutoff magnitude as the low-magnitude point of deviation from a straight line on a log frequency–magnitude diagram (Fig. 3), equivalent to a departure from the Gutenberg–Richter distribution (Gutenberg and Richter 1954). This definition of cutoff magnitude was chosen to balance the twin aims of retaining sufficient data to observe a signal whilst avoiding spurious results due to changes in catalogue completeness. In all cases, we repeated the analysis using a higher cutoff magnitude to test that the observed changes in VT pattern were indeed consistent. Using the low-magnitude point of deviation, therefore, the selected cutoff magnitudes are 2.5 and 2.1 for data recorded during 1960–1969 and 1969–1983, respectively. The true completeness magnitude is likely to be higher at times of high earthquake rate, owing to saturation of the seismic network (e.g., after a large-magnitude earthquake or during the initial stages of dyke injection (Kagan 2004)), but this effect is unlikely to influence our conclusions for the aspects of seismicity we study here.

The distribution of VT earthquakes

More than 90% of the VT earthquakes recorded between 1960 and 1983 occurred at depths less than or equal to 13 km, and the distribution of their hypocentres allows Kilauea's edifice to be divided into three distinct volumes (also described as primary seismic volumes), each of which is associated with specific volcanic processes (Klein et al. 1987a, b): (1) at depths less than or equal to 5 km beneath the summit caldera, which lies above an enduring shallow magma reservoir, the top of which is located at a depth of 3–4 km (Tilling and Dvorak 1993); (2) at depths less than or equal to 5 km within the rift-zones; and (3) at depths between 7 and 10 km beneath the mobile south flank. Earthquakes at depths greater than 13 km are associated

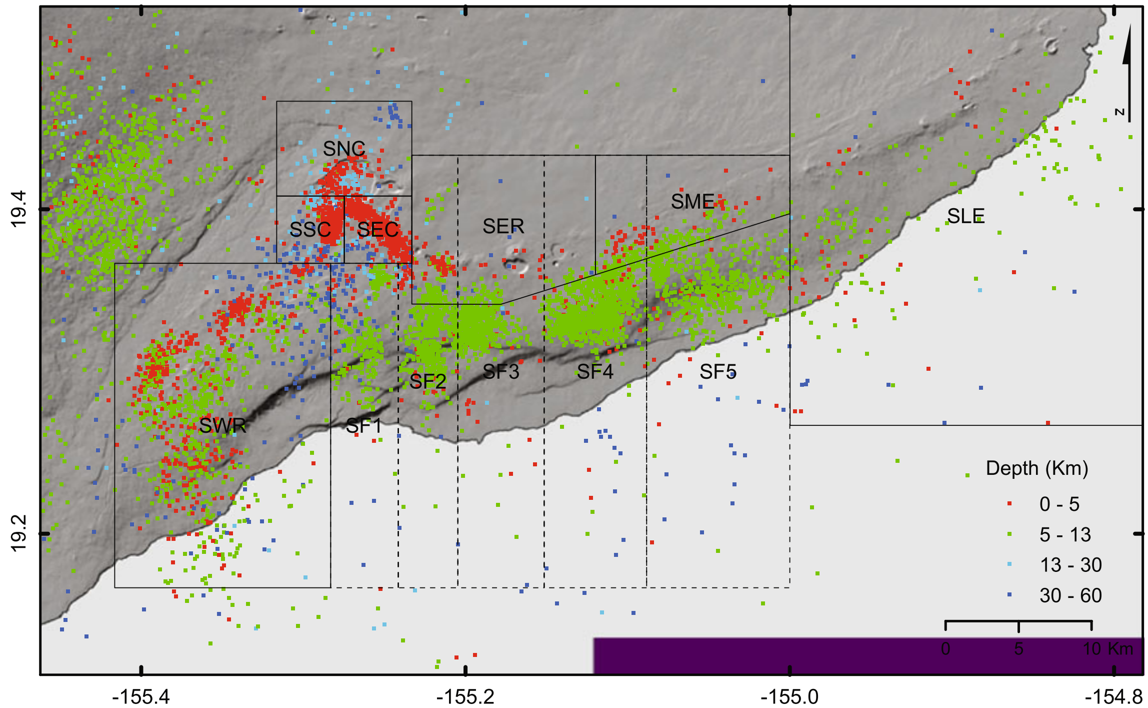

Fig. 1 Seismicity and HVO seismic regions of Kilauea volcano. *Coloured squares* indicate locations of VT earthquakes of magnitude 2.5 and greater that occurred between 1969 and 1983, with the hypocentre depth being indicated by the colour scale

with the supply of magma from depth (Ryan 1988). The uncertainty on the hypocentral locations is about 1–2 km, which is sufficiently small for the vast majority of earthquakes to have been allocated to the appropriate volume.

The three primary volumes have since been subdivided by the HVO into smaller seismic regions (Nakata 2006). Following the HVO subdivisions, our data can be grouped spatially as follows: (1) for the caldera, earthquakes at depths of less than 5 km in the shallow east, shallow west and shallow north caldera volumes; (2) for the rift-zones, earthquakes at depths of less than 5 km within the shallow east, shallow middle-east and shallow lower east rift-zones and south-west rift-zone volumes; and (3) for the south flank, earthquakes at depths between 5 and 13 km within the five south-flank volumes (SF1–SF5).

Characteristic sequences of VT earthquakes during magmatic unrest

The three primary seismic volumes display preferred patterns of VT earthquake rate with time (Fig. 4). The caldera and rift-zones are characterized by episodes with elevated earthquake rate separated by intervals with almost no earthquakes, whereas the south flank is characterized by a nearly steady rate of earthquake occurrence, occasionally punctuated by transient increases in earthquake rate.

An alternative set of characteristic patterns can be identified when the behaviour of VT earthquake rate is considered in relation to the onset of eruptions or intrusions. In this case, the patterns are not constrained from the outset to lie within a particular primary seismic volume (although they may show a preferred geographical location). On this basis, three further characteristic sequences can be identified, as follows.

Sequences of earthquakes for which the mean rate accelerates over time-scales of weeks to months. They occur below the caldera and frequently culminate in an eruption or intrusion, suggesting that they are the result of edifice deformation under elevated magma pressure.

The sudden onset of elevated rates of earthquakes, which then return to background values after a few hours or days. The rapid onset commonly coincides with the start of an eruption or intrusion. These sequences have been observed in the caldera and rift-zones and are associated with a migration of the hypocentres away from known magma reservoirs (Klein et al. 1987a, b; Rubin et al. 1998). The combined spatial and temporal patterns suggest that the sequences are associated with the shallow emplacement of dykes.

The sudden onset of elevated rates of earthquakes, followed by a gradual decay to background values after a few hours or days. These sequences can be distinguished from those observed in the caldera and rift-zones by the following features: The rapid onset may occur as much as 1 day before *or* after the eruption or intrusion; the hypocentres are located in the south flank, up to 10 km

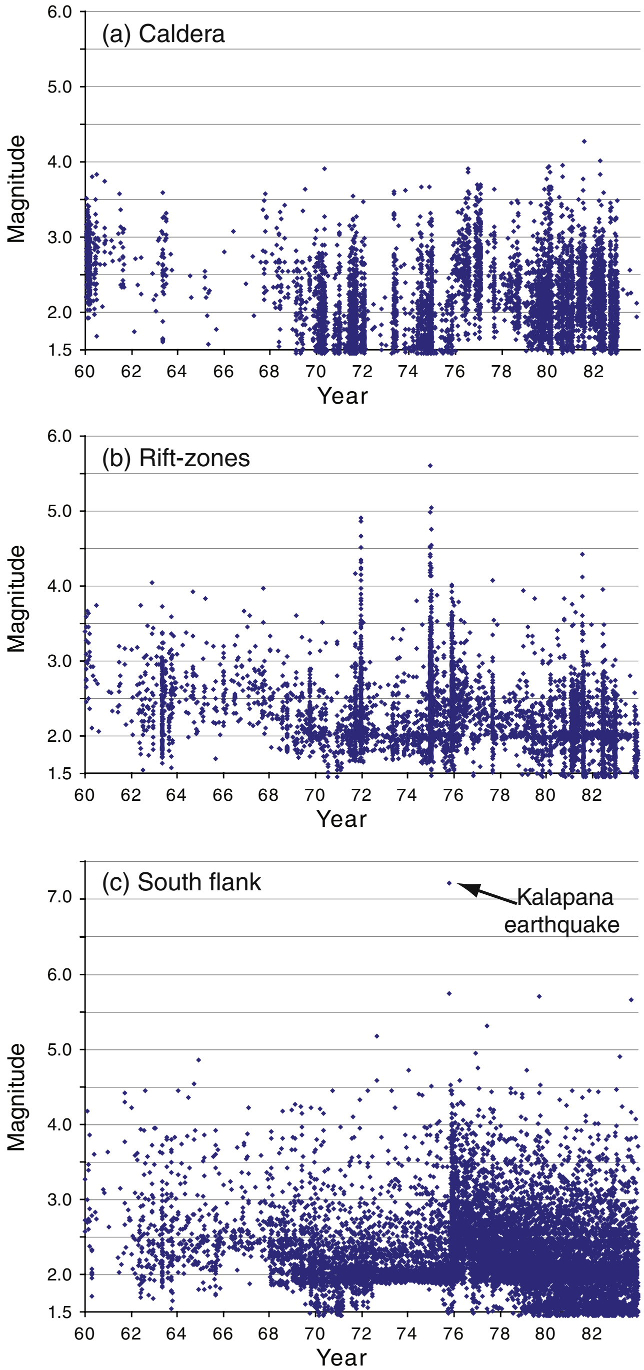

Fig. 2 Local magnitudes of VT earthquakes of magnitude 1.5 and greater recorded in the Hawaii Volcano Observatory catalogue for the caldera, rift-zones and south flank of Kilauea between 1960 and 1983

from the caldera and rift-zones; and the hypocentres show no systematic migration with time. The three distinguishing features suggest that these sequences may be related to a widespread instability of the flank, possibly through aseismic slip (Segall et al. 2006), rather than a localised response to magmatic processes.

These three sequences are investigated below, in order to identify connections between behaviour in the caldera region, rift-zones and south flank and, from these, to evaluate the potential for developing reliable short-term forecasts of eruptions.

Precursory sequences of VT earthquakes in the caldera

Final and intermediate eruptions

VT seismicity in the caldera is dominated by consecutive sequences of accelerating rates of earthquakes. Almost all of these sequences culminate in a reported magmatic event, whether an eruption or a dyke intrusion (Fig. 4). Of the 57 magmatic events between 1960 and 1983, a precursory increase in earthquake rate of more than a few hours in duration was identified in the caldera region before nine eruptions and nine intrusions. These precursory sequences were observed only from 1969 onwards. It is difficult to determine whether their absence before this date is due to a real change in behaviour or to the lower sensitivity of the network.

Two distinct relations can be identified among the 18 sequences for which a magmatic event was preceded by an accelerating rate of occurrence of VT earthquakes (Fig. 5). Thus, in 11 of the sequences, the eruption or intrusion was immediately followed by a drop in VT earthquake rate, which then remained at very low values for weeks to months. The eruptions or intrusions therefore occurred at the culmination of an accelerating sequence and so are defined as *final* magmatic events. In the remaining seven sequences, the eruption or intrusion occurred before the end of the increase in earthquake rate; in other words, the VT earthquake rate appears to continue increasing undisturbed by a magmatic event. Because the eruptions or intrusions

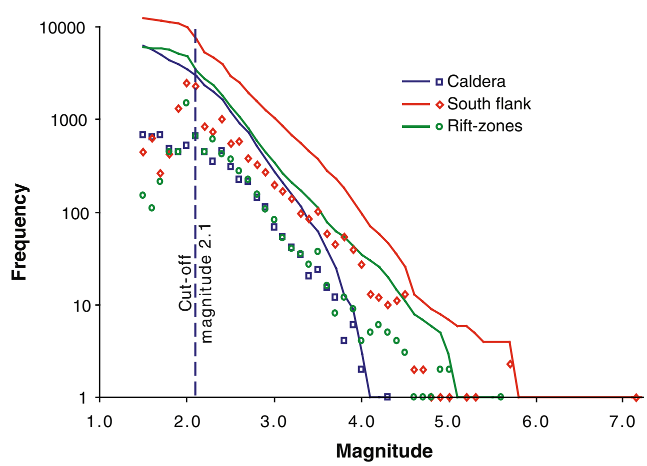

Fig. 3 Frequency–magnitude distribution for earthquakes recorded at the caldera, rift-zones and south flank regions of Kilauea between 1969 and 1983. *Solid lines* are the cumulative number of earthquakes of a given magnitude or larger; points are the discrete number of earthquakes of a given magnitude

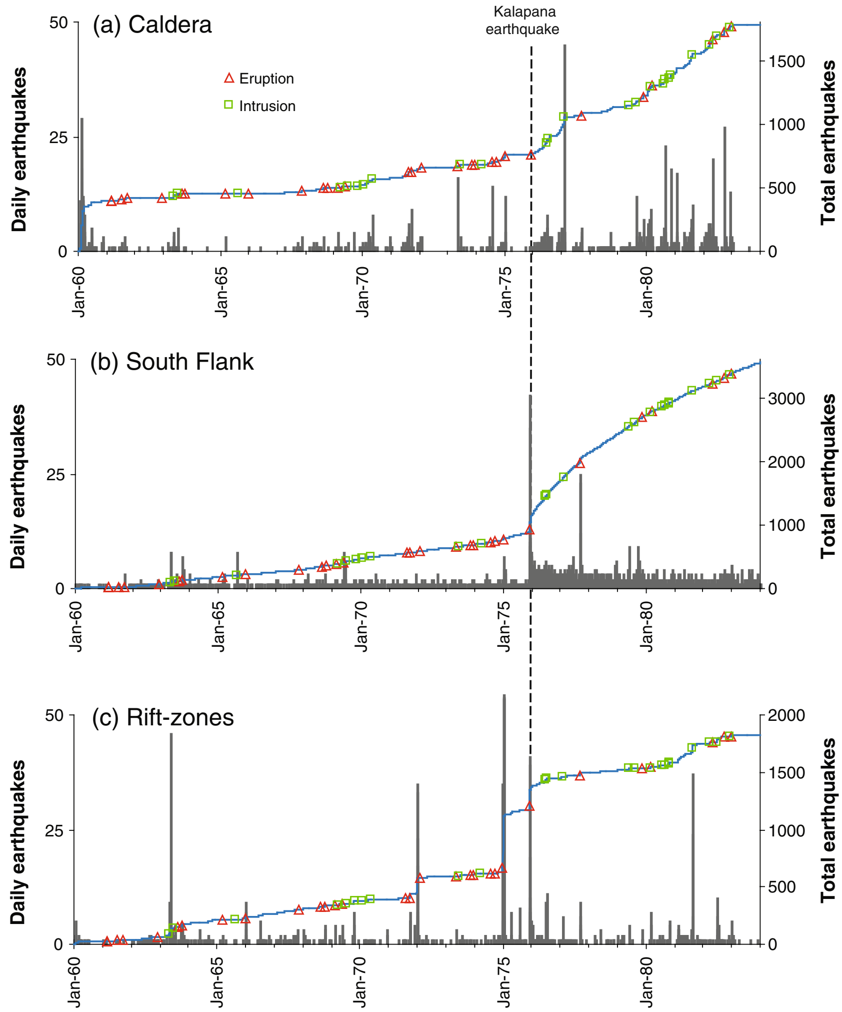

Fig. 4 Daily and cumulative total numbers of VT earthquakes of magnitude 2.5 and greater at the caldera, rift-zones and south flank regions of Kilauea between 1960 and 1983. Occurrence of eruptions and dyke intrusions indicated by *red triangles* and *green squares*, respectively

do not halt the increase in earthquake rate, they are defined as *intermediate* magmatic events. An intermediate magmatic event can then be followed by another intermediate or a final magmatic event.

Precursory sequences and ground deformation

Final and intermediate magmatic events are associated with different patterns of ground deformation at the caldera. Figures 5b and 6 compare trends in VT earthquake occurrence with changes in radial tilt at the summit, as recorded along an orientation of N60°W by daily measurements at a tiltmeter located at Uwekahuna on the northwest edge of the caldera (Lengliné et al. 2008). The data show that final magmatic events tend to be followed by significant subsidence at the caldera, whereas intermediate magmatic events are associated with little or no subsidence. Apparently, final events drain magma from the summit reservoir more quickly than it can be replaced by new magma from below, leading to subsidence at the summit. During intermediate events, however, magma continues to be supplied to the reservoir as quickly as magma escapes (in eruption or as a dyke intrusion outward from the reservoir), so that associated changes in ground deformation are small.

In all but one of the sequences in Fig. 6, the amount of summit tilt continued to increase until a final eruption. The exception is the decrease in summit tilt that occurred between the final eruption on 8 February 1977 and the preceding intermediate event on 14 July 1976 (Fig. 6d). After the first 20% of the interval had been completed, the summit tilt subsided by about 40 microradians between 25 August and 30 September 1976, before resuming its inflation until the final eruption. The deflation is inferred to reflect a migration of magma into a fracture that failed to propagate as a typical rift-zone dyke. Notably, it was accompanied by an interruption of VT seismic activity until re-inflation had recovered about 60% of its value before subsidence began (Fig. 6d). Almost immediately, the VT earthquake rate resumed the value it had attained before caldera subsidence, rather than accelerating gradually from long-term background rates. Such a pattern suggests that

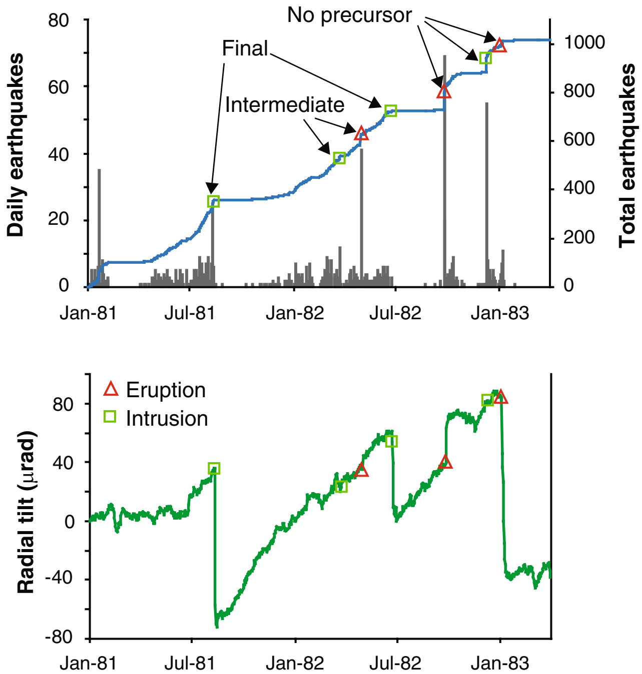

Fig. 5 (*Top*) Daily and cumulative total numbers of VT earthquakes of magnitude 2.1 and greater and (*bottom*) radial tilt for Kilauea caldera between 1981 and 1983

fracturing could resume only after the edifice had approached the strain it had achieved before caldera subsidence. Similar behaviour, known as the Kaiser effect, has been observed during rock deformation experiments in the laboratory (Main and Meredith 1991), and so it may be a common feature of deformation and fracturing at volcanoes that are subjected to alternating episodes of increasing and decreasing loading.

Quantifying accelerations in rates of VT seismicity

Accelerations in VT earthquake rate are anticipated to follow an exponential or power-law trend with time (Voight, 1988). To distinguish between trends, we have used the maximum-likelihood techniques of Ogata (2006) to fit exponential and power-law trends with a Poisson distribution of earthquake rate uncertainties (Marsan and Nalbant 2005) and a Bayesian Information Criterion (BIC) for model preference (Bell et al. 2011). We fit a power-law acceleration of the form $(t_f - t)^{-p}$and an exponential acceleration of the form $\exp[-\lambda(t_f - t)]$, where t_f is the time of the eruption or intrusion and p and λ are the power-law and exponential parameters, respectively. We then validate the resultant fits by considering the rates, which should be randomly scattered within some confidence interval. When both exponential and power-law models are valid, we evaluate the BIC to decide whether it is possible to identify a preferred model. The BIC is given by $\mathrm{BIC} = -2\log(L) + P\log(n)$ where L is the likelihood of the observations for the given model, P is the number of free parameters and n is the number of observations.

Figure 7 shows the best-fit power-law and exponential models of the earthquake rates for the seven precursory sequences in Fig. 6, along with an additional modified sequence preceding the 8 February 1977 event, where the 74 days of quiescence associated with summit subsidence are cut from the original sequence (Fig. 7, d-ii). Although the sequences show significant fluctuations in the earthquake rate about the mean trend, these typically fall within the 95% Poisson confidence limits. The sequence and model parameters, including BIC values are given in Table 1. For all eight sequences, the exponential model is preferred; frequently, the distribution of residuals invalidates the power-law model (i.e., they are systematically above or below the model trend), and in all instances, the BIC is lower for the exponential model. The edited 8 February 1977 sequence is much better modeled by an exponential function, confirming that the earthquake rates are identical before and after the deflation–inflation episode. The characteristic time-scales for the exponential acceleration $\tau = 1/\lambda$ range from 17 to 330 days (Table 1).

Eruptions, intrusions and seismicity in the south flank

Exponential and power-law increases in the rate of VT earthquakes with time are consistent with the approach to eruption or intrusion being controlled by the rate of development of fracture networks in the crust or volcanic edifice (Kilburn and Voight 1998; Kilburn 2003). As described above, only 17 out of 57 eruptions and intrusions recorded at Kilauea between 1960 and 1983 were preceded by such accelerating rates of VT earthquakes. A question therefore remains as to what mechanism governed the onset of the remaining magmatic events.

Evidence from recent eruptions at Mt Etna suggests that dyke intrusions and eruptions can be directly triggered by slip of a volcano's flank, even in the absence of an increase in magma pressure (Burton et al. 2005). In addition, continuous GPS measurements at Kilauea since the mid-1990s have identified transient episodes of aseismic slip within the south flank, many of which are accompanied by short-lived increases in the rate of small south-flank VT earthquakes (Brooks et al. 2006; Segall et al. 2006). We here analyze the rates of VT earthquakes occurring in the south flank of Kilauea between 1960 and 1983 in order to investigate the potential for transient slip to trigger eruptions and intrusions.

Figure 8a shows the daily rate of VT earthquakes located within the south flank of Kilauea between 1960 and 1983, along with the occurrence of eruptions and intrusions. We

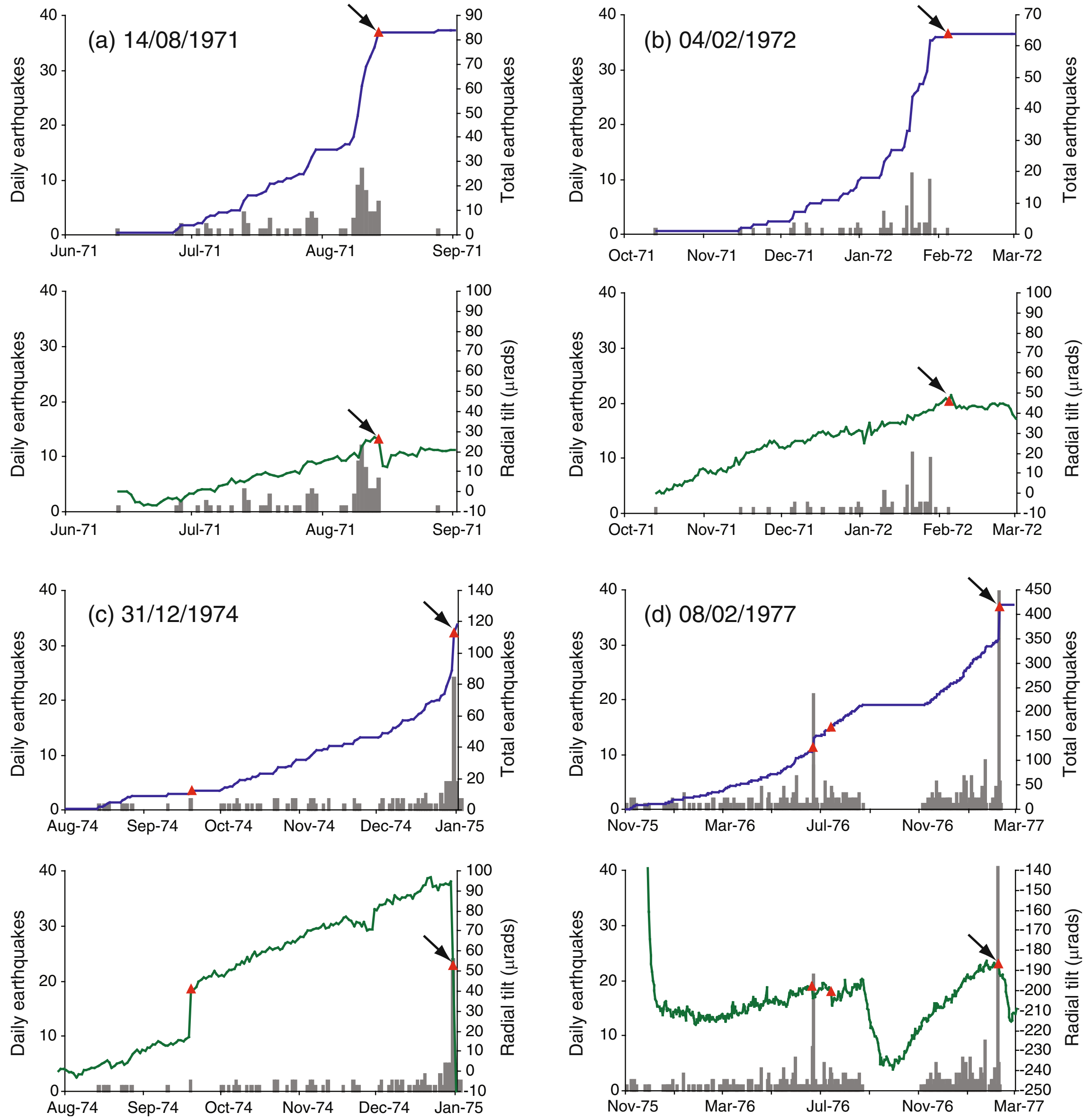

Fig. 6 Daily and cumulative total numbers of caldera VT earthquakes and surface radial tilt associated with final eruptions and intrusions at Kilauea (*arrowed*). Eruptions and intrusions are indicated by *red triangles*. Figure parts correspond to those in Fig. 7 and Table 1, and the dates of final magmatic events are: **a** 14 Aug 1971; **b** 04 Feb 1972; **c** 31 Dec 1974; **d** 08 Feb 1977; **e** 10 Mar 1980; **f** 10 Aug 1981; **g** 22 Jun 1982

use magnitude 2.5 and greater earthquakes, with hypocentres located at depths between 5 and 13 km in HVO regions SF1-5 (Section "VT earthquakes at Kilauea"). Very similar results are obtained using different magnitude cut-offs and when a 3-km exclusion buffer is applied surrounding the caldera and rift-zones to exclude any earthquakes that may have been wrongly located in the south flank. Initial inspection of Fig. 8a highlights how elevated rates of flank earthquakes coincide closely with the onset of magmatic events. Between January 1960 and November 1975, all days with four or more magnitude 2.5 or greater flank earthquakes coincide with the onset of an eruption or intrusion. However, following the magnitude 7.2 Kalapana earthquake in November 1975 the mean rate of south-flank earthquakes increases, and the interpretation of the daily number of earthquakes becomes more complicated.

The effect of changing mean rate of earthquakes can be accommodated by adopting a normalized measure of the departure from background conditions. A simple and well-established measure is the so-called Z-score, defined as $Z = \frac{(DER-\mu)}{\sigma}$ (Abdi and Salkind 2007), where *DER* is the measured daily earthquake rate, μ is the mean value of *DER* for a specified time interval, and σ is the standard deviation of the daily earthquake rate from the mean. The Z-score thus measures the number of standard deviations

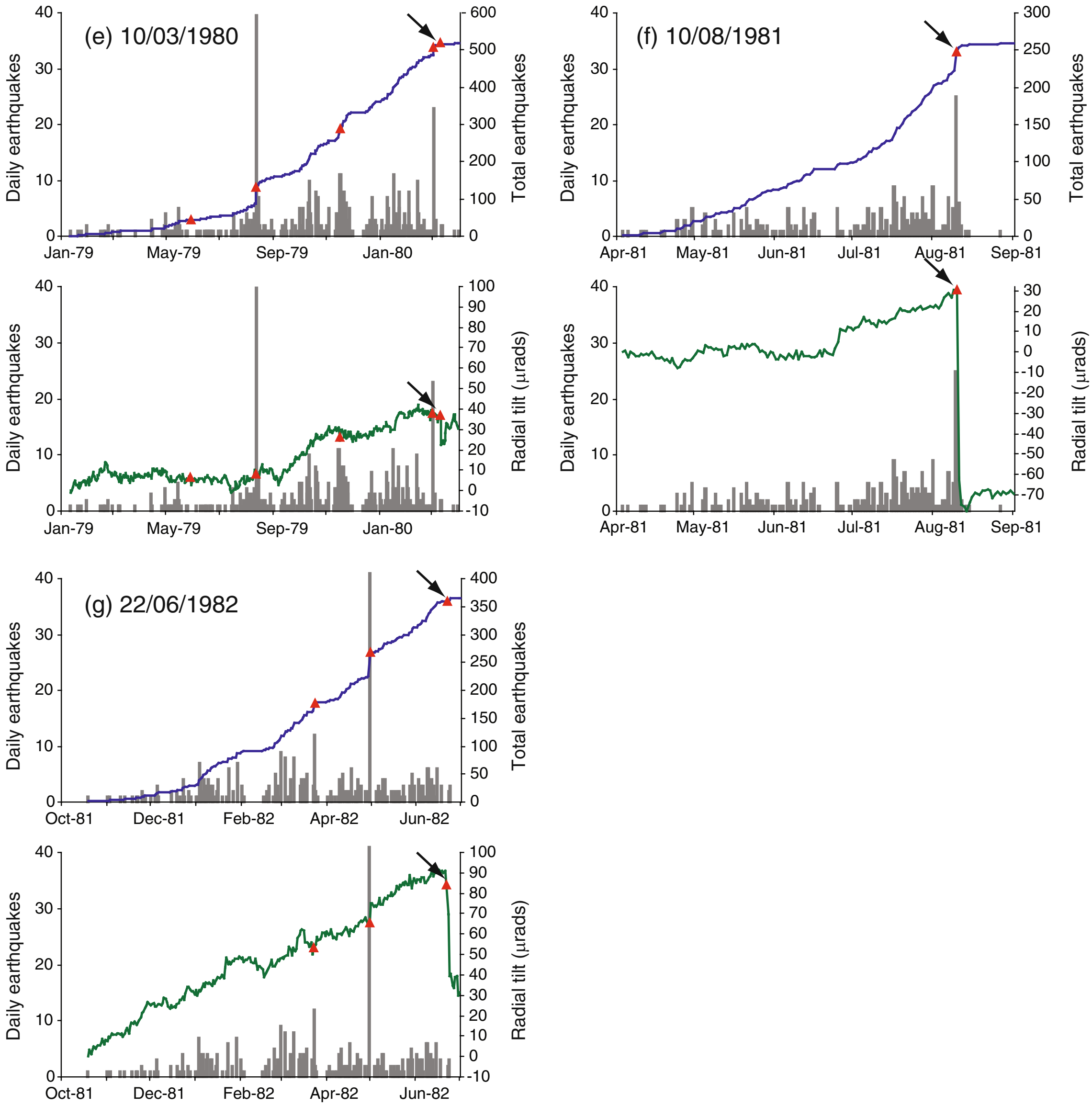

Fig. 6 (continued)

that the daily earthquake rate is from the mean, so that larger values indicate greater departures from the mean rate. Because μ and σ vary with time, they are estimated from a moving time window. Only minor differences occur for time windows with lengths between 20 and 500 days, and so a 50-day window has been chosen to illustrate the results.

Figure 8b shows the Z-scores for the daily rate of south-flank VT earthquakes with magnitudes of 2.5 or more. The values vary from −1 to about 70; negative Z-scores correspond to days with fewer events than the mean daily rate. Inspection of the distribution of Z-scores reveals a clear separation between high and low values (Fig. 8b). In addition, both before and after the Kalapana earthquake, the occurrence of Z-scores higher than 10 corresponds almost uniquely to the occurrence of magmatic events. We designate as a south-flank earthquake swarm any day with four or more south-flank earthquakes with magnitude 2.5 or greater and a daily Z-score of 8.0 or greater. Ten events meet such criteria and are reported in Table 2. Only the swarm on 22 September 1979 does not also coincide with a reported eruption or intrusion.

The coincidence of eruptions and intrusions with the highest daily rates of VT earthquakes with magnitudes of at least 2.5 and with the highest Z-scores indicates a strong coupling between volcanic activity and flank seismicity. However, the causality in this relation remains unclear; does volcanic activity trigger flank slip, or does flank slip trigger volcanic activity? We attempt to constrain the causality by looking in detail at the temporal evolution of caldera, rift-zone and south-flank seismicity associated with

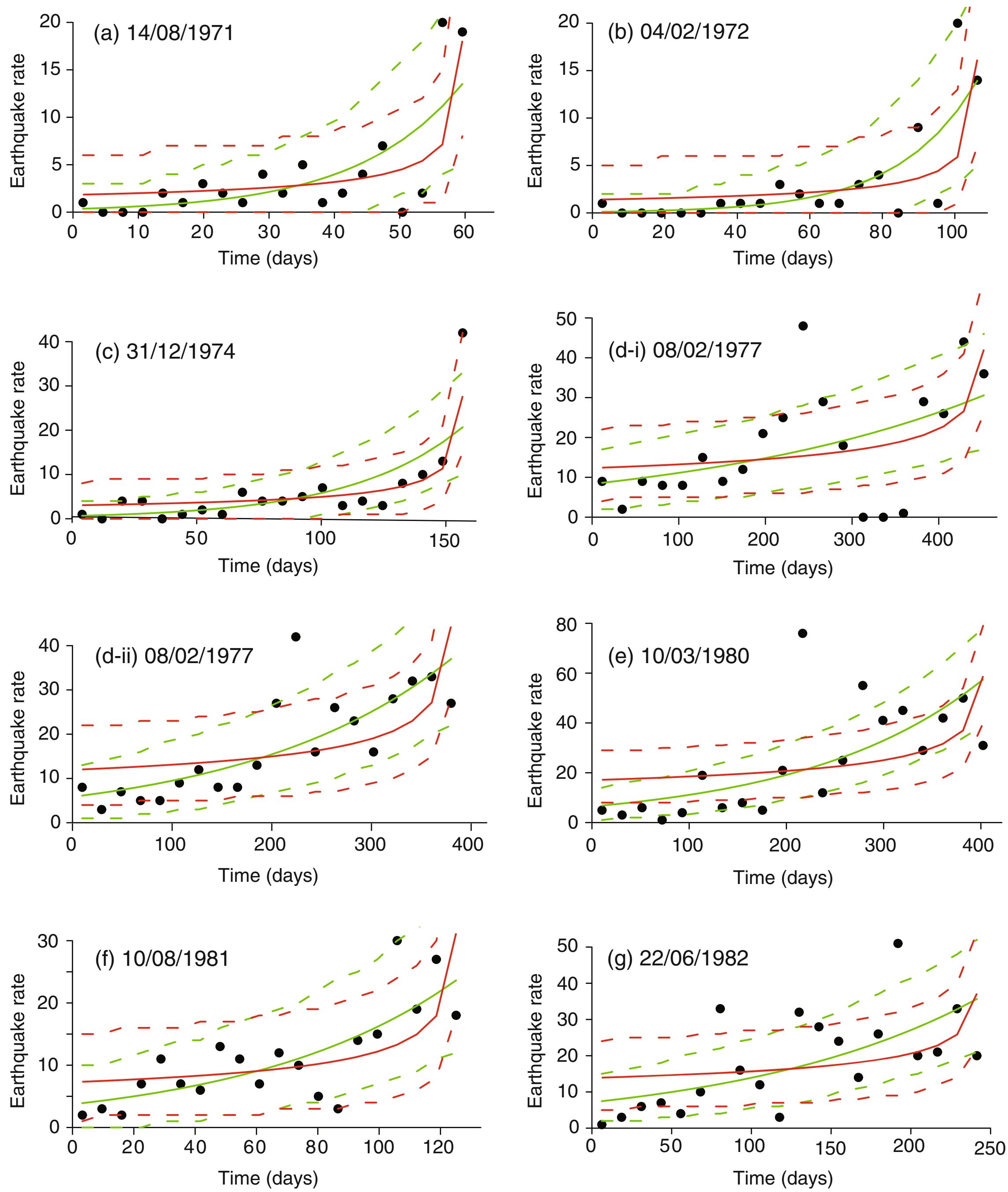

Fig. 7 Best-fit power-law and exponential models for the accelerating sequences of earthquakes shown in Fig. 6. Figure parts correspond to those in Fig. 6 and in Table 1; parts *d-i* and *d-ii* correspond to the entire sequence preceding the 08 Feb 1977 eruption, and the edited sequence (omitting the episode of quiescence), respectively. *Black dots* are data points, *red solid* and *dashed lines* show the best-fit power-law model and 95% confidence limits, respectively, and *green solid* and *dashed lines* show the best-fit exponential model and 95% confidence limits, respectively

the south-flank earthquake swarms. For example, if flank slip was responsible for triggering reservoir failure, with or without dyke injection, we might expect to see elevated rates of flank seismicity beginning before corresponding increases in the caldera and rift-zones.

For each of the ten south-flank swarms, the total number of earthquakes as a function of time for the caldera, rift-zones and south-flank regions are shown in Fig. 9. For the 24/08/1965, 29/05/1979 and 01/10/1983 events (Fig. 9c, h and j), there are too few earthquakes in the caldera and rift-zones to be sure of a relation. For the 31/12/1974 event (Fig. 9e), the onset of elevated rates of earthquakes in the caldera and rift-zone is at least 24 h before that in the south flank. For the 09/05/1963, 24/05/1969 and 12/09/1977 events (Fig. 9a, d and g), the onset of high rates of south-flank earthquakes approximately coincides with that

Table 1 Eruptions and intrusions at Kilauea between 1960 and 1983 that were preceded by episodes of accelerating rates of VT earthquakes located in the caldera

Event date	Figs. 6 and 7	Event type	Duration (days)	λ (1/days)	τ (days)	BIC_{exp}	p Value	BIC_{pl}	$\Delta BIC_{exp\text{-}pl}$
14 Aug 1971	(a)	Eruption	61	0.060	17	34	0.52	42	−8
04 Feb 1972	(b)	Eruption	109	0.050	20	64	0.55	79	−15
31 Dec 1974	(c)	Eruption	161	0.020	50	115	0.51	127	−12
08 Feb 1977	(d-i)	Intrusion	464	0.003	330	435	0.29	436	−1
08 Feb 1977	(d-ii)	Intrusion	390	0.005	200	351	0.31	371	−20
10 Mar 1980	(e)	Eruption	413	0.010	100	329	0.30	385	−56
10 Aug 1981	(f)	Intrusion	128	0.010	100	81	0.34	88	−7
22 Jun 1982	(g)	Intrusion	248	0.010	100	197	0.24	221	−24

λ is the maximum-likelihood exponential constant, $\tau=1/\lambda$ is the characteristic exponential timescale, p is the maximum-likelihood power-law constant, and BIC_{exp}, BIC_{pl}, and $\Delta BIC_{exp\text{-}pl}$ are the values of the Bayesian Information Criterion for the exponential and power-law models, and their difference, respectively

in either the caldera or rift-zones. For the 05/10/1963 and 29/11/1975 (Kalapana earthquake) events (Fig. 9b and f) the onset of elevated flank seismicity is slightly before the onset of elevated caldera or rift-zone seismicity. The 22 September 1979 south-flank swarm (Fig. 9i) was not associated with a magmatic event but was initiated by a large (magnitude 5.7) earthquake in the south flank. In summary, there is no simple relation between the timing of the onset of high rates of earthquakes in the caldera, rift-zone and south-flank regions during these events.

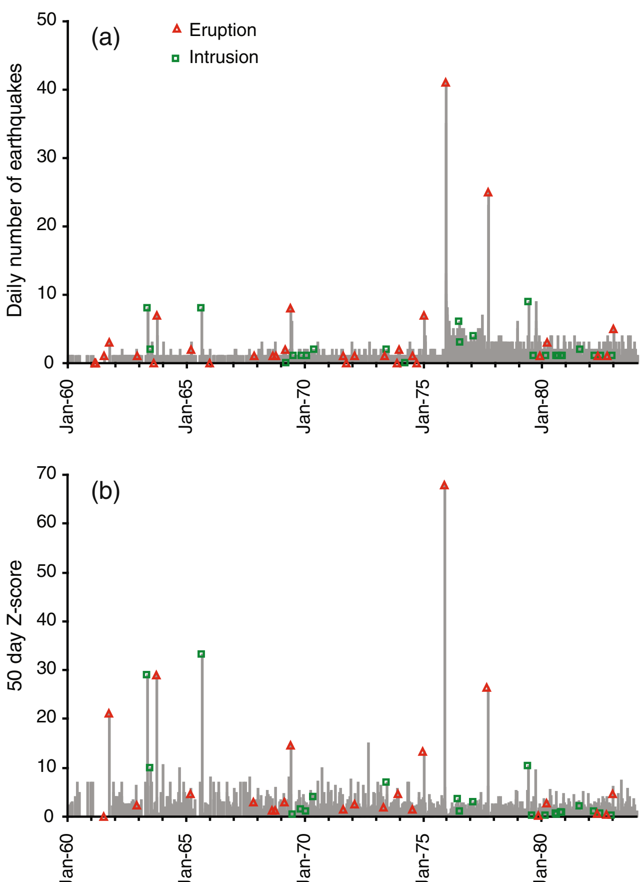

Fig. 8 **a** Daily number of earthquakes and **b** Z-score for the daily number of earthquakes based on a 50-day moving window of VT earthquakes of magnitude 2.5 and greater located in the south flank of Kilauea. Volcanic eruptions are indicated by the *red triangles*, intrusions by the *green squares*

Discussion

Precursory sequences of caldera VT earthquakes

The sequences of caldera earthquakes with an accelerating mean rate preceding eruptions and intrusions are best attributed to fracturing in rock before the propagation of a dyke from a pressurized magma reservoir beneath the

Table 2 South flank earthquake swarms at Kilauea between 1960 and 1983

Swarm date	Fig. 9	Event type	N_{SF}	Acceleration	M_{max}
09 May 1963	(a)	Intrusion	20	No	3.7
05 Oct 1963	(b)	Eruption	14	No	3.8
24 Aug 1965	(c)	Intrusion	9	No	3.9
24 May 1969	(d)	Eruption	10	No	3.5
31 Dec 1974	(e)	Eruption	14	Yes	4.5
29 Nov 1975	(f)	Eruption	96	No	7.2
12 Sept 1977	(g)	Eruption	63	No	4.2
29 May 1979	(h)	Intrusion	14	No	3.2
22 Sept 1979	(i)	None	19	No	5.7
01 Jan 1983	(j)	Eruption	10	No	3.9

N_{SF} is the total number of magnitude 2.5 or greater south flank VT earthquakes occurring within 4 days of the start of the swarm; "Acceleration" indicates whether or not the swarm was preceded by an acceleration of the rate of caldera earthquakes (see Table 1), and M_{max} is the magnitude of the largest south flank earthquake during the swarm

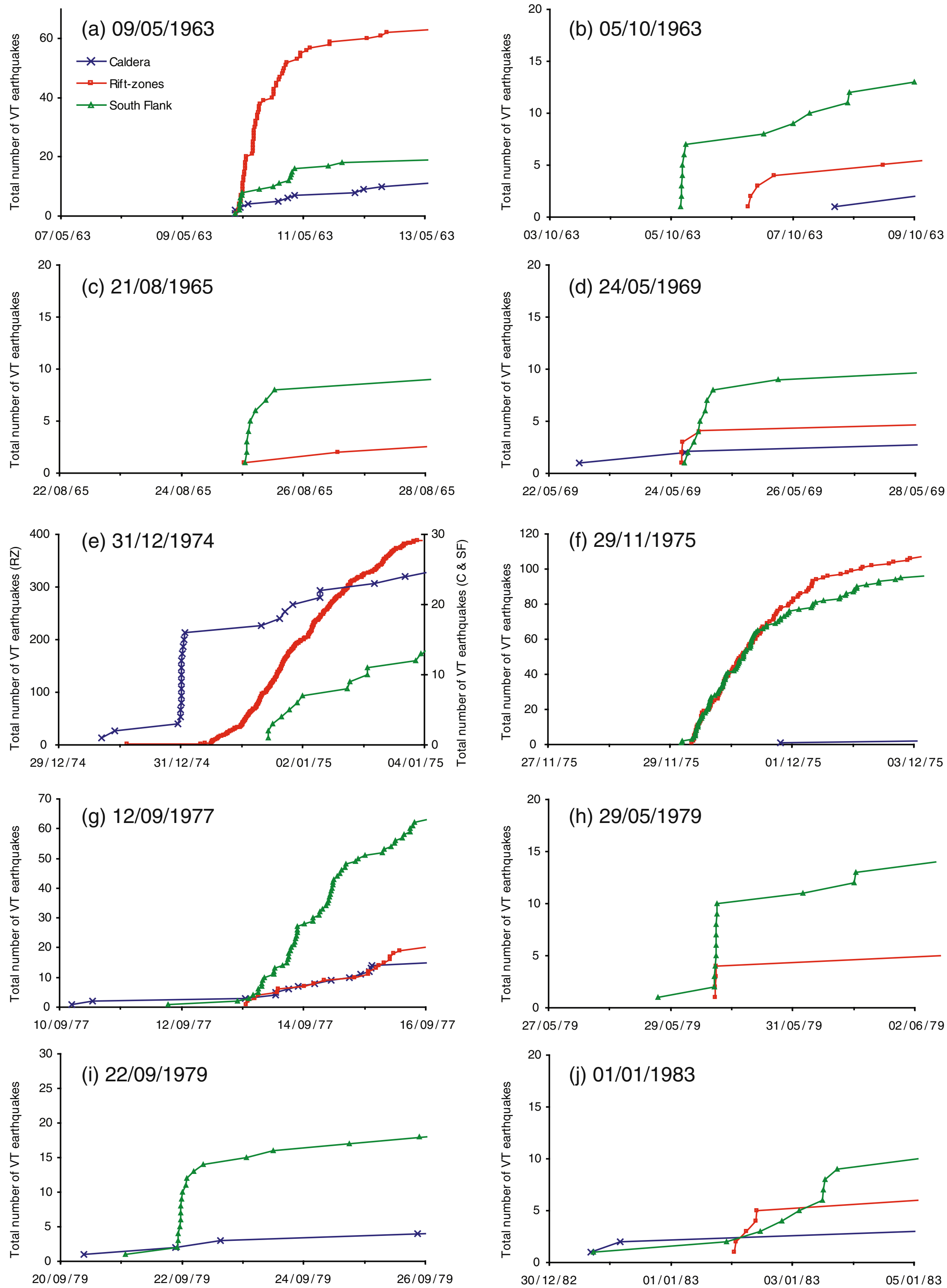

Fig. 9 The variation with time in number of VT earthquakes of magnitude 2.5 and greater associated with south flank swarms at Kilauea between 1960 and 1983. Note the second *Y*-axis on Fig. 9e to accommodate the large number of rift-zone earthquakes for this event

summit (Tilling and Dvorak 1993). The fracturing conditions identify only the approach to the injection of a dyke and do not constrain whether or not a dyke will reach the surface. The approximately constant rate of surface deformation during the sequences suggests that the bulk strain rate is constant, even when the VT earthquake rate accelerates with time. A non-linear relation is thus indicated between strain rate and the rate of brittle fracturing.

Our maximum-likelihood fitting demonstrates that an exponential model for the accelerating mean rate of VT earthquakes is preferred to a power-law model. An exponential trend contains no internal constraint on the maximum VT event rate (or total number of VT events) before bulk fracturing is expected; the event rate will be expected to increase without limit (Voight 1988). To forecast the time of bulk failure, therefore, an external constraint must be applied on the maximum rate of VT precursors.

In practice, exponential trends are considered to reach uncontrolled conditions when the parameter they are describing exceeds about 100 times its initial value (Jaeger 1969). Applied to VT earthquakes, uncontrolled conditions are expected when the mean rate increases to about 100 times the starting rate in previously unstressed rock. Such uncontrolled conditions, in turn, are associated with the formation of a fracture across the volume of the volcano being deformed (Kilburn 2003). However, from inspection of Fig. 7, eruption or intrusion occurs after only a five- to tenfold increase in the rate of VT earthquakes. Hence, either the precursory sequences develop in pre-stressed crust (so that the observed start rate does not correspond to unstressed conditions), or dykes can propagate before fracturing produces a through-going discontinuity.

For a dyke to propagate, the hydro-fracture criterion, $p_e \geq \sigma_3 + T_0$, must be locally satisfied, where p_e is the excess magma pressure (total magma pressure−lithostatic pressure), σ_3 is the minimum principal compressive stress and T_0 is the tensile strength of the rock (Gudmundsson 2006; Gudmundsson and Philipp 2006). Dyke injection can therefore be enabled by (1) an increase in magma pressure, (2) a decrease in the local minimum compressive stress (e.g., due to gravitational spreading of a volcano's flanks or stress redistribution near the reservoir), or (3) a reduction in the tensile strength of the rock (e.g., through chemical corrosion). All three mechanisms may operate in the caldera region of Kilauea, and, as a result, it may prove difficult to extract reliable eruption forecasts from VT earthquake data alone. A more promising route, to be investigated in future work, may be a combined analysis of seismic and strain data.

Volcanic activity in the absence of precursory accelerations in the rate of caldera earthquakes

Between 1960 and 1983, the eruptions and intrusive events analyzed here all appear to have involved the opening of a magma pathway through some part of the volcanic edifice. Creation of a new pathway requires fracturing and, hence, the onset of VT seismicity. It is thus remarkable that only 18 of the 57 magmatic events were preceded by prolonged accelerations in the rate of VT earthquakes. Of the remaining 40 events, nine occurred in association with earthquake swarms in the south flank (Table 2), whereas 31 appear to have occurred without either prolonged VT earthquake sequences in the caldera or swarms in the south flank.

Eruptions associated with south-flank earthquake swarms

The almost unique coincidence of south-flank earthquake swarms with dyke-fed eruptions and intrusions (Table 2) provides strong evidence of an interaction between the flank and the magmatic system. The rapid onset and transient nature of the swarms further suggests that the interaction involves a rapid stress change in the south flank. Such a stress change may be induced either by a change in magma pressure in the dyke itself, or by a transient increase in the rate of flank slip, which then favours contemporaneous dyke injection and an earthquake swarm in the south flank.

Several studies have proposed that flank slip is normally induced by dyke injection (Dvorak et al. 1986; Cayol et al. 2000; Klein et al. 2006). However, the alternative view is supported by the eruption associated with the magnitude 7.2 Kalapana earthquake in November 1975, when the estimated 7.1 m of flank slip promoted dyke injection into both rift-zones, which widened by 3–5 m (Owen and Burgmann 2006). In this case, it was possible to determine the relative timing of flank slip and eruption owing to the large magnitude of the Kalapana earthquake. It is possible, therefore, that smaller movements (which promote small-magnitude earthquakes, some of which may be too small to be detected) associated with slow-slip earthquakes could also promote south-flank swarms and dyke injection. Indeed, eight of the ten south-flank swarms recorded between 1960 and 1983 were associated with an eruption, and, of these, only once (on 31 December 1974) was the eruption also preceeded by an increase in the rate of VT earthquakes beneath the main shallow magma reservoir (Table 2). Finally, one south-flank swarm occurred without detected magmatic activity (22 September 1979).

The observation that south-flank swarms can occur without magmatic activity indicates that south-flank movements cannot automatically be attributed to dyke intrusion. In addition, the association of most south-flank swarms with eruptions without prolonged VT precursors suggests that the eruptions occurred through crust that was already close to bulk failure. As a result, a reduction in confining stress (σ_3) due to south-flank movements may have been sufficient to favour the rapid onset of dyke propagation (without prolonged increases in VT earthquake rate) from the main shallow magma reservoir. Such an interpretation is consistent with recent observations using continuous GPS stations on the south flank of Kilauea (Brooks et al. 2006; Brooks et al. 2008). These observations confirm that slow-slip earthquakes can occur with or without magmatic events, so that magmatic activity may be a response to, rather than a trigger of, slow-slip earthquakes.

Eruptions not associated with south-flank earthquake swarms

More than half of the eruptions and intrusions at Kilauea between 1960 and 1983 occurred without either prolonged increases in VT earthquake rate or earthquake swarms in the south flank (following Sequence 3 in Section "VT earthquakes at Kilauea"). At the same time, these magmatic events appear to have required the formation of a newly connected fracture system to act as a pathway for magma transport. The absence of prolonged sequences of precursory VT earthquakes thus suggests that the crust was already close to conditions for completing a new through-going fracture (e.g., from the caldera into the rift-zones), such that VT earthquakes occurred as a local swarm in the rift-zones during the final formation of the pathway immediately before or during magma transport. Such an interpretation is consistent with the crust around the caldera and rift-zones remaining under stress after a previous eruption. As a result, only a modest increase in magma pressure or modest decrease in confining pressure would be required to trigger an eruption or intrusion. Neither condition would have involved prolonged precursors. Hence, an eruption could rapidly be triggered either by the arrival of magma into the shallow reservoir or by a reduction in crustal stress due to an amount of flank movement insufficient to generate a south-flank swarm of earthquakes.

Implications for eruption forecasting

Three types of precursory sequence have been recognized before eruptions and intrusions at Kilauea between 1960 and 1983—30% of eruptions and intrusions were preceded by prolonged increases in VT earthquake rate in the caldera; 15% were preceded only by earthquake swarms in the south flank, and 55% were preceded only by local earthquake swarms related to magma being transported through the rift-zones. Hence, 70% of eruptions and intrusions are associated only with swarms during or immediately before the event. In other words, more than two volcanic events in three cannot be forecast using prolonged increases in VT seismicity alone.

The range of precursory sequences can be related to the amount of strain already accumulated in the caldera region before the onset of bulk fracturing and magma transport. When the accumulated strain is low, prolonged precursors are observed while the applied stress and strain increase (e.g., due to an increase in magma pressure) to the point of bulk failure. When the accumulated strain is already close to that for bulk failure, only a small change in strain is required to trigger a magmatic event. The small change may be produced by a reduction in confining stress due to slow-slip of the south flank, or by an increase in magma pressure, due to the arrival of new material from depth or to the onset of vesiculation. In all cases, the precursory sequences cannot be used to distinguish between the approach to an eruption or an intrusion.

When prolonged sequences of VT earthquake precursors occur in the caldera, they are characterised by exponential increases in mean earthquake rate with time. Such increases can be used to forecast an eruption only if another criterion can also be applied to relate conditions for an eruption to a critical VT earthquake rate or total number of recorded earthquakes. Until such a criterion becomes available, the data indicate an empirical constraint that an eruption is most likely when the mean event rate reaches five to ten times its value at the start of the precursory sequence.

Conclusions

Fifty-seven eruptions and intrusions occurred at Kilauea between 1960 and 1983, after which the volcano has been in a state of virtually continuous eruption. About one third of eruptions and intrusions were preceded by prolonged increases in VT earthquake rate in the caldera, about one sixth were preceded only by earthquake swarms in the south flank, and just over one half were preceded only by local earthquake swarms related to magma being transported through the rift-zones.

In combination, the results indicate that, at Kilauea: (1) VT seismicity on its own is not sufficient either to guarantee a reliable short-term forecast of a magmatic event, or to distinguish between the approach to an eruption or intrusion; (2) forecasts could be improved by combining changes in VT earthquake rate with changing conditions of strain in the crust; and (3) slow-slip of the south flank is a potential trigger of eruptions, rather than a response to magmatic events.

They also suggest that flank instability may be an important control on the timing of magmatic events and, through its influence on strain distribution within the volcano, also on the style of precursory sequences. Similar conditions may also apply at large, frequently erupting basaltic volcanoes with unstable flanks, such as Mt. Etna, in Sicily and Piton de la Fournaise on Reunion Island.

Improved knowledge of the absolute states of the excess magma pressure, confining stress and the tensile strength of the crust, together with models of how they evolve with time (through processes such as magma recharge and time-dependent deformation) will be required before uncertainties in forecasts can be reduced.

Acknowledgments This research was funded by the UK Natural Environment Research Council (AFB). During writing, AFB was funded by the European Commission NERIES and TRIGS projects. We thank the USGS Hawaiian volcano observatory for access to the Hawaiian earthquake catalogue, John Greenhough for helpful discussion, and two anonymous reviewers for their constructive comments and suggestions.

References

Abdi H, Salkind NJ (2007) Z-scores. Encyclopedia of measurement and statistics. Sage, Thousand Oaks, CA

Bell AF, Greenhough J, Heap MJ, Main IG (2011) Challenges for forecasting based on accelerating rates of earthquakes at volcanoes and laboratory analogues. Geophys J Int. doi:10.1111/j.1365-246X.2011.04982.x

Brooks BA, Foster J, Sandwell D, Wolfe CJ, Okubo P, Poland M, Myer D (2008) Magmatically triggered slow slip at Kilauea volcano, Hawaii. Science 321:1177. doi:10.1126/science.1159007

Brooks BA, Foster JH, Bevis M, Frazer LN, Wolfe CJ, Behn M (2006) Periodic slow earthquakes on the flank of Kilauea volcano, Hawai'i. Earth Planet Sci Lett 246(3–4):207–216. doi:10.1016/j.epsl.2006.03.035

Burton MR, Neri M, Andronico D, Branca S, Caltabiano T, Calvari S, Corsaro RA, Del Carlo P, Lanzafame G, Lodato L, Miraglia L, Salerno G, Spampinato L (2005) Etna 2004–2005: An archetype for geodynamically-controlled effusive eruptions. Geophys. Res. Lett. 32(9) doi:10.1029/2005GL022527

Cayol V, Dieterich JH, Okamura AT, Miklius A (2000) High magma storage rates before the 1983 eruption of Kilauea, Hawaii. Science 288(5475):2343–2346

Chastin SFM, Main IG (2003) Statistical analysis of daily seismic event rate as a precursor to volcanic eruptions. Geophys. Res. Lett. 30(13) doi:10.1029/2003GL016900

Collombet M, Grasso JR, Ferrazzini V (2003) Seismicity rate before eruptions on Piton de la Fournaise volcano: implications for eruption dynamics. Geophys Res Lett 30(21). doi:10.1029/2003GL017494

De la Cruz-Reyna S, Reyes-Davila GA (2001) A model to describe precursory material-failure phenomena: applications to short-term forecasting at Colima volcano. Mexico Bull Volcanol 63(5):297–308

Delaney PT, Denlinger RP, Lisowski M, Miklius A, Okubo PG, Okamura AT, Sako MK (1998) Volcanic spreading at Kilauea, 1976–1996. J Geophys Res- Solid Earth 103(B8):18003–18023

Dvorak JJ, Okamura AT, English TT, Koyanagi RY, Nakata JS, Sako MK, Tanigawa WT, Yamashita KM (1986) Mechanical response of the south flank of Kilauea Volcano, Hawaii, to intrusive events along the rift systems. Tectonophys 124(3–4):193–209

Gudmundsson A (2006) How local stresses control magma-chamber ruptures, dyke injections, and eruptions in composite volcanoes. Earth-Sci Rev 79(1–2):1–31. doi:10.1016/j.earscirev.2006.06.006

Gudmundsson A, Philipp SL (2006) How local stress fields prevent volcanic eruptions. J Volc Geotherm Res 158(3–4):257–268. doi:10.1016/j.jvolgeores.2006.06.005

Gutenberg B, Richter CF (1954) Seismicity of the earth and associated phenomena. Princeton University Press, Princeton

Jaeger JC (1969) Elasticity, fracture and flow. CRC Press, Boca Raton

Kagan YY (2004) Short-term properties of earthquake catalogs and models of earthquake source. Bull Seismol Soc Amer 94 (4):1207–1228

Kilburn CRJ (2003) Multiscale fracturing as a key to forecasting volcanic eruptions. J Volcanol Geotherm Res 125(3–4):271–289

Kilburn CRJ, Voight B (1998) Slow rock fracture as eruption precursor at Soufriere Hills volcano. Montserrat Geophys Res Lett 25 (19):3665–3668

Klein FW (1984) Eruption forecasting at Kilauea Volcano, Hawaii. J Geophys Res 89(NB5):3059–3073

Klein FW, Koyanagi RY, Nakata JS, Tanigawa WR (1987a) The seismicity of Kilauea's magma system. In: Decker RW, Wright TL, Stauffer PH (eds) Volcanism in Hawaii., pp 1019–1185

Klein FW, Koyanagi RY, Nakata JS, Tanigawa WR, Decker RW, Wright TL, Stauffer PH (1987) The seismicity of Kilauea's magma system. In: Volcanism in Hawaii. USGS Professional Paper 1350; pp 1019–1185

Klein FW, Wright T, Nakata J (2006) Aftershock decay, productivity, and stress rates in Hawaii: indicators of temperature and stress from magma sources. J. Geophys. Res-Solid Earth 111(B7)

Lengliné O, Marsan D, Got JL, Pinel V, Ferrazzini V, Okubo PG (2008) Seismicity and deformation induced by magma accumulation at three basaltic volcanoes. J. Geophys. Res-Solid Earth 113(B12):12 doi:10.1029/2008JB005937

Main IG (2000) A damage mechanics model for power-law creep and earthquake aftershock and foreshock sequences. Geophys J Int 142(1):151–161

Main IG, Meredith PG (1991) Stress-corrosion constitutive laws as a possible mechanism of intermediate-term and short-term seismic quiescence. Geophys J Int 107(2):363–372

Marsan D, Nalbant SS (2005) Methods for measuring seismicity rate changes: a review and a study of how the M-w 7.3 Landers earthquake affected the aftershock sequence of the M-w 6.1 Joshua Tree earthquake. Pure Appl Geophys 162(6–7):1151–1185. doi:10.1007/s00024-004-2665-4

McGuire WJ, Kilburn CRJ (1997) Forecasting volcanic events: some contemporary issues. Geol Rundsch 86(2):439–445

McNutt SR (1996) Seismic monitoring and eruption forecasting of volcanoes: a review and state-of-the-art and case histories. In: Scarpa R, Tilling RI (eds) Monitoring and mitigation of volcano hazards. Springer, Berlin, pp 99–146

Moran SC (2003) Multiple seismogenic processes for high-frequency earthquakes at Katmai National Park, Alaska: evidence from stress tensor inversions of fault-plane solutions. Bull Seismol Soc Amer 93(1):94–108

Nakata J (2006) Hawaiian volcano observatory seismic data, January to December 2005: U.S. Geological Survey Open-File Report 2006–1103: pp 122

Ogata Y (2006) Statistical analysis of seismicity–updated version (SASeis2006). Computer Science Monographs 33

Owen SE, Burgmann R (2006) An increment of volcano collapse: kinematics of the 1975 Kalapana, Hawaii, earthquake. J Volcanol Geotherm Res 150(1–3):163–185

Reyes-Davila GA, De la Cruz-Reyna S (2002) Experience in the short-term eruption forecasting at Volcan de Colima, Mexico, and public response to forecasts. J Volc Geotherm Res 117(1–2):121–127

Roman DC, Cashman KV (2006) The origin of volcano-tectonic earthquake swarms. Geology 34(6):457–460. doi:10.1130/g22269.1

Rubin AM, Gillard D, Got JL (1998) A reinterpretation of seismicity associated with the January 1983 dike intrusion at Kilauea Volcano, Hawaii. J Geophys Res-Solid Earth 103(B5):10003–10015

Ryan MP (1988) The mechanics and 3-dimensional internal structure of active magmatic systems—Kilauea Volcano, Hawaii. J. Geophys. Res-Solid Earth and Planets 93(B5):4213–4248

Segall P, Desmarais EK, Shelly D, Miklius A, Cervelli P (2006) Earthquakes triggered by silent slip events on Kilauea volcano, Hawaii. Nature 442(7098):71–74. doi:10.1038/nature05297

Smith R, Kilburn CRJ, Sammonds PR (2007) Rock fracture as a precursor to lava dome eruptions at Mount St Helens from June 1980 to October 1986. Bull Volcanol 69(6):681–693. doi:10.1007/s00445-006-0102-5

Soosalu H, Einarsson P, Porbjarnardottir BS (2005) Seismic activity related to the 2000 eruption of the Hekla volcano. Iceland Bull Volcanol 68(1):21–36. doi:10.1007/s00445-005-0417-7

Sparks RSJ (2003) Forecasting volcanic eruptions. Earth Planet Sci Lett 210(1–2):1–15. doi:10.1016/S0012-812X(03)00124-9

Tilling RI, Dvorak JJ (1993) Anatomy of a basaltic volcano. Nature 363(6425):125–133

Tokarev PI (1971) Forecasting volcanic eruptions from seismic data. Bull Volcanol 35:243–250

Voight B (1988) A method for prediction of volcanic-eruptions. Nature 332(6160):125–130

Zobin VM (2003) Introduction to volcanic seismology. Elsevier, Amsterdam